Title

Cortical spreading depression produces long-term disruption of activity-related changes in cerebral blood volume and neurovascular coupling

Journal

Journal of Biomedical Optics, 10(1)

ISSN

1083-3668

Authors

Guiou, Michael
Sheth, Sameer
Nemoto, Masahito
et al.

Publication Date

2005

Peer reviewed

Cortical spreading depression produces long-term disruption of activity-related changes in cerebral blood volume and neurovascular coupling

Michael Guiou
Sameer Sheth
Masahito Nemoto
Melissa Walker
Nader Pouratian
Alyssa Ba
Arthur W. Toga
University of California, Los Angeles, School of Medicine
Department of Neurology
Laboratory of Neuro Imaging
Los Angeles, California 90024
E-mail: toga@loni.ucla.edu

Abstract. Cortical spreading depression (CSD) is a pronounced depolarization of neurons and glia that spreads slowly across the cortex followed by a period of depressed electrophysiological activity. The vascular changes associated with CSD are a large transient increase in blood flow followed by a prolonged decrease lasting greater than 1 h. Currently, the profile of functional vascular activity during this hypovolemic period has not been well characterized. Perfusion-based imaging techniques such as functional magnetic resonance imaging (fMRI) assume a tight coupling between changes in neuronal and vascular activity. Under normal conditions, these variables are well correlated. Characterizing the effect of CSD on this relationship is an important step to understand the impact acute pathophysiological events may have on neurovascular coupling. We examine the effect of CSD on functional changes in cerebral blood volume (CBV) evoked by cortical electrophysiological activity for 1 h following CSD induction. CBV signal amplitude, duration, and time to peak show little recovery at 60 min post-induction. Analysis of spontaneous vasomotor activity suggests a decrease in vascular reactivity may play a significant role in the disruption of normal functional CBV responses. Electrophysiological activity is also attenuated but to a lesser degree. CBV and evoked potentials are not well correlated following CSD, suggesting a breakdown of the neurovascular coupling relationship.
 [DOI: 10.1117/1.1852556]

Keywords: cortical spreading depression; neurovascular coupling; optical imaging.

Paper NEU-11 received Feb. 23, 2004; revised manuscript received May 1, 2004; accepted for publication Aug. 11, 2004; published online Feb. 1, 2005.

1 Introduction

Cortical spreading depression (CSD) is a pronounced depolarization of neurons and glia that spreads across the cortex at a rate of 3 to 5 mm/min followed by a prolonged period of depressed cortical activity.[1] Clinically, CSD is postulated to play a role in the pathogenesis of stroke,[2] traumatic cortical injury,[3] cerebral ischemia,[4,5] migraine,[6] and transient global amnesia.[7] CSD can be induced by a variety of stimuli including pinprick or needle stab,[8,9] elevated potassium,[5,10] electrical stimulation,[1,11] or glutamate application. On a cellular level, electrophysiological changes are accompanied by significant shifts in intra- and extracellular ion concentrations,[12] cellular swelling,[13] dendritic beading,[14] and changes in gene expression.[15] The vascular changes associated with CSD are a large transient increase in blood flow[16] followed by a prolonged period of decreased flow lasting[17,18] greater than 1 h. These large flow-related phenomena have been observed using a variety of techniques including laser Doppler flowmetry[8] (LDF), positron emission tomography[19] (PET), functional magnetic resonance imaging[20] (fMRI), and optical imaging of intrinsic signals[21,22] (OIS). Since first described by Leão in 1994, a large focus of CSD research has aimed at elucidating the mechanism mediating the CSD event itself. Relatively fewer studies have sought to assess the long-term effect of CSD on functional brain activity. Widely used perfusion-based functional imaging techniques such as fMRI and PET assume a tight coupling between changes in neuronal activity and the ensuing vascular response. In light of the significant impact of CSD on global vascular function, a characterization of the effect of spreading depression on activity-related perfusion signals is of utmost importance to test the stability of the neurovascular coupling relationship in pathophysiological conditions in which CSD is thought to play an important role.

OIS is a functional imaging technique that measures wavelength-dependent changes in cortical light reflectance induced by changes in hemoglobin (Hb) concentration, cell swelling, and light scattering.[23,24] The technique is well-suited for functional brain mapping as it permits the simultaneous mapping of large regions of cortex with high spatial (in micrometers) and temporal (in milliseconds) resolution.[24–26] Utilizing wavelengths of light where oxyhemoglobin (HbO_2)

Address all correspondence to Dr. Arthur W. Toga, Laboratory of NeuroImaging, 710 Westwood Plaza, Suite 4-238, Mail Code 176919, Los Angeles, CA 90024-1769. Tel: 310-206-2101; Fax: 310-206-5518; E-mail: toga@loni.ucla.edu

1083-3668/2005/$22.00 © 2005 SPIE

and deoxyhemoglobin (Hbr) absorb equally (506, 522, 549, 569, and 586 nm) enables the monitoring of total hemoglobin concentration or cerebral blood volume[24,27] (CBV). Under normal conditions, stimulus-induced changes in CBV are robust and correlate well with changes in neuronal activity,[28] making it an ideal measure to assess the effects of CSD on functional vascular signals and neurovascular coupling. In this paper, we examine the effect of CSD on (1) evoked cortical electrophysiological and vascular activity and (2) the neurovascular coupling relationship.

2 Methods

2.1 *Animal Preparation*

Seven male Sprague-Dawley rats (Charles River Laboratories) weighing 200 to 400 g were studied in accordance with University of California at Los Angeles (UCLA) Animal Research Committee guidelines. Subjects were initially anesthetized with halothane in 40% O_2-60% N_2 (5% induction; 1.5% during surgery) and placed in a stereotaxic apparatus (David Kopf Instruments, Tujunga, California). Anesthetic depth was assessed by periodically monitoring the toe pinch withdrawal reflex, eyeblink reflex, and respiratory rate. Core body temperature was maintained at 37 ± 0.5°C with a rectal probe and homeothermic heating blanket (Harvard Apparatus, Holliston, Massachusetts). The head was shaved and a midline incision was made, after which the underlying tissue was dissected and retracted. The skull over the right parietal bone was thinned with a manual scraping instrument (Biomedical Research Instruments, Rockville, Maryland) until the middle cerebral artery and superior cerebral veins were clearly visible ($\sim$250 μm). Two burr holes were drilled approximately 3 mm apart in the skull under high magnification for electrophysiological recording and CSD induction. Special attention was paid to avoid large cortical vessels in both burr hole sites. Following completion of surgery, animals were switched to enflurane anesthesia (1 to 1.5%) for the remainder of the experiment. Imaging began at least 1 h after the discontinuation of halothane and completion of the surgical preparation.

2.2 *Optical Imaging*

The stereotactic frame was mounted to the stage of a Nikon SMZ1500 microscope. Light was provided by a voltage-stabilized halogen light source (PL900 Dolan Jenner, Lawrence, Massachusetts) and guided through a filter wheel (Lamda 10-2, Sutter Instruments, Novato, California) to provide filtered incident light upon the preparation. For this experiment, light was filtered at 570 nm (FWHM 10), to emphasize changes in CBV. Images were acquired with a 16-bit, slow-scan Princeton Instruments TE/CCD-576EFT CCD camera (Princeton Instruments, Trenton, New Jersey). The field of view covered 8.6×6.4 mm with 192×144 pixels providing a resolution of $\sim$43 μm/pixel. Data were stored on a PC running a LabView (National Instruments, Austin, Texas) virtual instrument to simultaneously collect OIS and electrophysiological data. Images were acquired at 1 Hz, with an exposure time of 100 ms. One stimulation trial consisted of 47 s of imaging. Stimulation began 13 s after the start of the trial, followed by a 2-s electrical stimulation to the left hindpaw. Individual stimulations were separated by 1 min. Ten pre-CSD trials were run to establish a functional baseline. Following CSD induction, optical signals were recorded for 3 min. Sixty trials (one per minute) were run during the post-CSD period.

2.3 *Electrical Stimulation*

For electrical stimulation, stainless steel needle electrodes (0.01 inch diameter, 8-deg tip, A-M systems, Carlsborg, Washington) were inserted into the hindpaw, one in the plantar surface of the foot and the other several millimeters away on the medial aspect of the leg. Electrical pulses (1 mA, 1 ms duration) were delivered at 5 Hz via a constant current source (Pulsar 6bp, FHC, Bowdoinham, Maine). Previous data from our lab have shown these simulation parameters produce a robust CBV response with no attenuation of individual evoked responses.[29]

2.4 *CSD Induction*

CSD was induced via cortical pinprick with a 27-gauge tuberculin needle inserted to a depth of $\sim$500 μm below the surface of the cortex.

2.5 *Electrophysiology*

Extracellular field potentials were recorded simultaneously with optical images by a low-impedance microelectrode (0.7 MΩ at 1 kHz, 125-μm shaft diameter, 12-deg tip, A-M Systems) advanced to a depth of $\sim$500 μm. The analog signals were amplified 1000 times using an eight-channel isolation amplifier (SCXI 1120, National Instruments, Austin, Texas), low-pass filtered at 10 kHz, and sampled at 1 kHz. Data were acquired for the first 18 s of the trial covering the 13-s baseline and 2-s stimulation. A reference electrode was inserted midline in the fascia just caudal to the surgical site. The electrophysiological and imaging setup was enclosed in a Faraday cage to reduce electromagnetic interference. Electrode position was determined using a combination of stereotactic coordinates and activation data collected at 570 nm prior to insertion. The electrode was inserted under high magnification to ensure clean penetration.

2.6 *Data Analysis*

Data analysis was carried out on a UNIX Silicon Graphics workstation running a series of Matlab (The Mathworks, Hollister, Massachusetts) programs written in-house. Optical data were analyzed using a ratio method that provides signal change in terms of fractional change from baseline. Briefly, ratio images were generated by first subtracting every image in a trial by an average of all prestimulus images (baseline) for that trial and then dividing each of these subtraction images by the baseline. Pre-CSD trials were averaged for each animal. Post-CSD stimulation trials were separated into 10-min time bins. Trials within a bin were averaged providing six post-CSD time points ($t_1=1$ to 10 min, $t_2=10$ to 20 min, $t_3=20$ to 30 min, $t_4=30$ to 40 min, $t_5=40$ to 50 min, and $t_6=50$ to 60 min). Responses at each post-CSD time point were averaged across animals and compared to the group average of pre-CSD values.

For each subject, we compared OIS signal amplitude, timing, and duration between pre- and post-CSD trials. Signal amplitude was calculated in a 1.0 mm diameter circular region of interest (ROI). An automated program (Matlab) determined

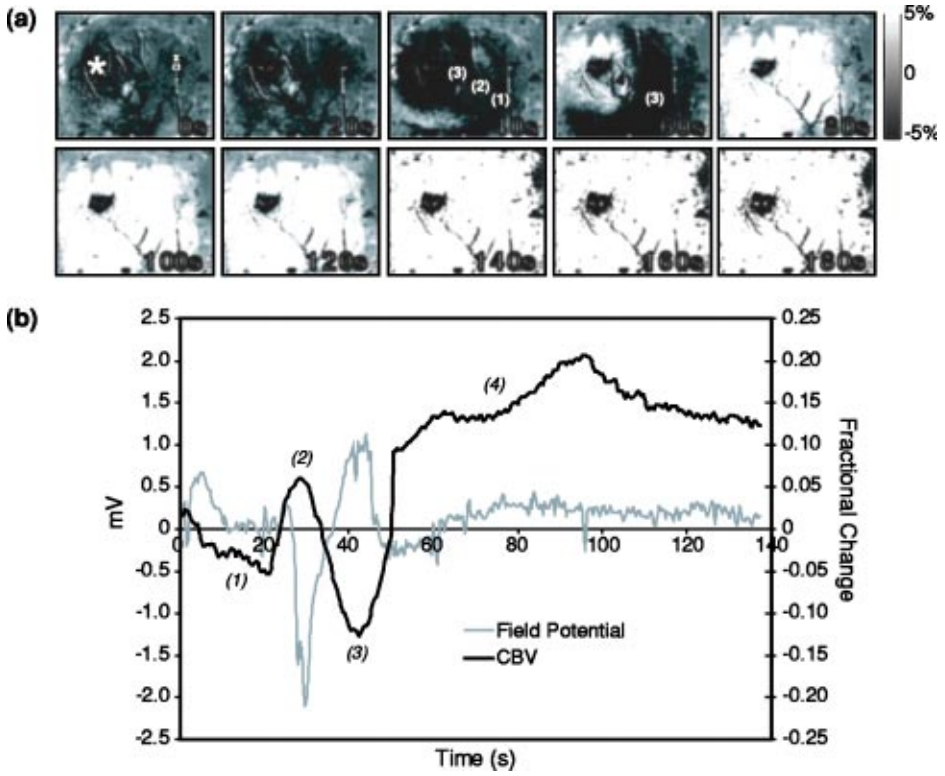

Fig. 1 Evolution of the CSD response. (a) Panels show ratio images taken under 570-nm illumination from a single animal. Induction site is marked with a white asterisk (*). Electrode insertion point is marked with a white circle (○). A white × shows the approximate location of the ROI used to calculate the OIS intensity timecourse. The OIS response showed a four-phase profile. Phases are marked in parentheses in image panels corresponding to 40 and 60 s post-induction. (b) Time plot of OIS and field potential changes of CSD event depicted in (a). The four phases of the CSD response shown in (a) are labeled. Initial OIS changes (phases 1 and 2) roughly coincide with the large negative deflection of the field potential, suggesting early optical changes associated with CSD may arise from physiological changes associated with the large depolarizing wave of electrical activity. Phases 3 and 4 are shown to correspond to an increase then decrease in blood volume using intravascular dye imaging.[22] These large-scale changes mirror the large increase then decrease in blood flow measured using flow sensitive techniques.

the 1.0 mm diameter circular region that produced the maximal response in the average of pre-CSD ratio images 2 to 3 s following stimulation for each rat. The temporal profiles of responses were characterized by calculating response onset and offset time (time to FWHM during the rise and fall of the response, respectively) and duration [(offset time)-(onset time)].

OIS changes associated with CSD were calculated in a small ROI (10×10 pixels) placed adjacent to the electrode burr hole. This position enabled us to compare the timing of OIS and electrophysiological changes associated with the CSD response.

Electrophysiological data were analyzed as follows. An evoked field potential consisted of an initial large negative deflection followed by a smaller positive potential. We first measured the amplitude of each evoked response from baseline to the initial negative peak and then averaged these values to create a sum evoked potential (ΣEP) for that trial. By accounting for every EP in a trial, ΣEP is a measure of the total neuronal activity evoked by the stimulation.[30,31] For each rat, pre-CSD ΣEPs were averaged and compared to the average of each post-CSD time bin.

Optical and electrophysiological responses during the post-CSD period were compared using a correlation analysis. Peak CBV responses were plotted against ΣEP in a scatter plot. A least-squares regression analysis provided an R^2 and a P value for the correlation.

3 Results

3.1 *CSD*

CSD produced a four-phase optical response [Fig. 1(a)]. Two initial small-amplitude phases of decreased (6.3±4.9%) then increased (2.5±1.7%) reflectance spread out concentrically from the induction site at a rate of ~3.5 mm/min. These two phases can be clearly seen at 40 s in the upper row of Fig. 1(a) and in the intensity plot in Fig. 1(b). These initial changes were followed by a large amplitude decrease (14.4±7%) then increase (13.4±7.5%) in reflectance that can be seen at 60 and 80 s in Fig. 1(a). The late reflectance increase persisted throughout the CSD imaging run in each animal. This prolonged decrease in the optical signal can be seen in the intensity plot in Fig. 1(b).

3.2 *Functional Changes Following CSD: CBV, ΣEP, and Amplitude*

Stimulus-induced CBV activations were a monophasic decrease in reflectance. The amplitude of pre-CSD responses was 0.071±0.003. Following CSD, the amplitudes of CBV

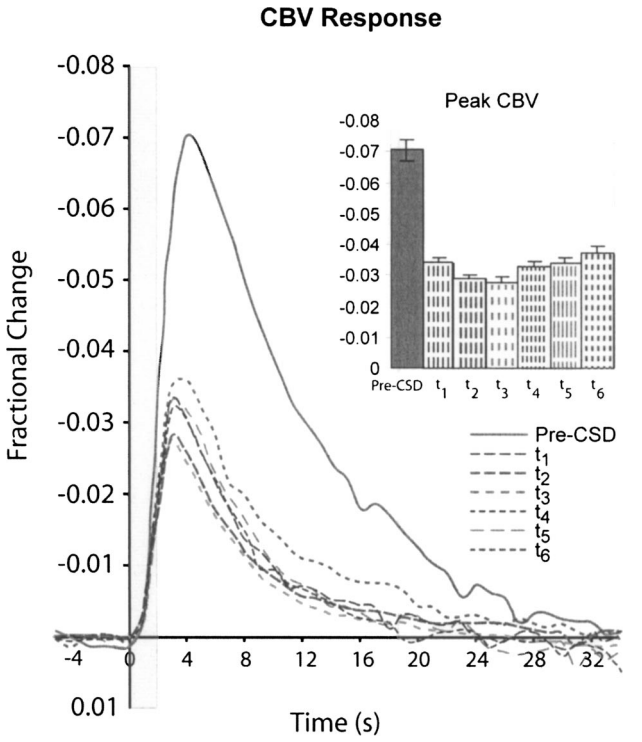

Fig. 2 Activity-related changes in CBV. CBV response to hindpaw stimulation produced a monophasic decrease in reflectance. Intensity time plots of pre- and post-CSD time points show a significant attenuation in response amplitude and duration following CSD. Shaded green region indicates stimulus duration. Inset shows the peak CBV values for pre- and post-CSD time points. Values reached a minimum at 20 to 30 min following CSD induction with only minimal recovery by 60 min. Error bars represent standard error.

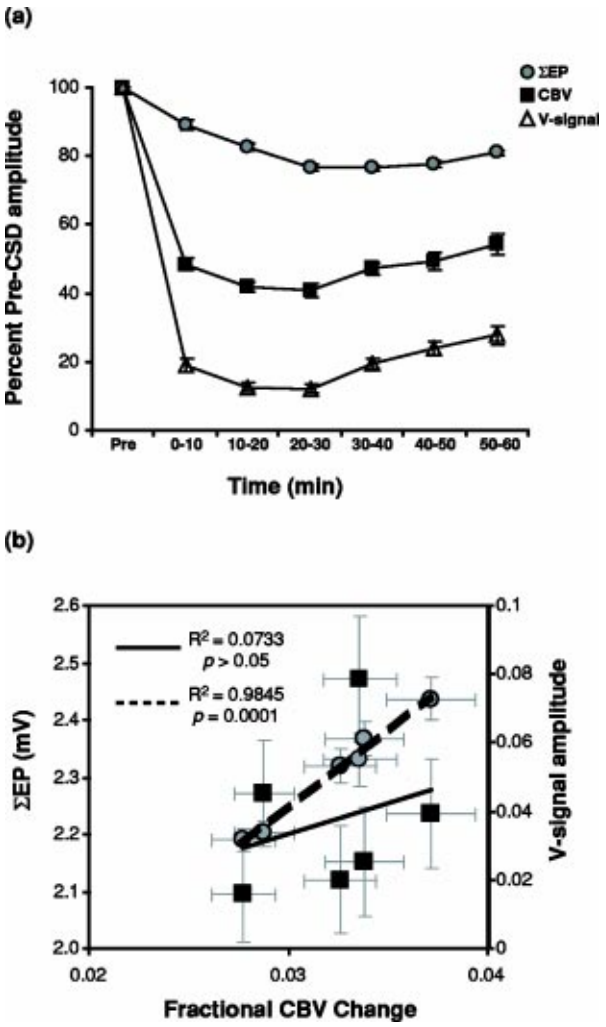

Fig. 3 (a) Normalized plot of peak values for CBV, ΣEP, and 0.1-Hz vasomotion signal (V-signal). Functional CBV signals were more significantly affected by CSD than ΣEP. Values show the greatest divergence during the first 30 min following induction. V-signal amplitude was significantly reduced during the post-CSD period. The profile of V-signal and functional CBV response amplitude closely paralleled each other. Error bars represent standard error. (b) Scatter plot of peak ΣEP and V-signal amplitude versus functional CBV responses during the post-CSD period. Linear regression analysis showed functional CBV and ΣEP were not well correlated ($R^2=0.073$, $P>0.05$), suggesting a breakdown of neurovascular coupling. Under normal conditions, functional CBV amplitude and ΣEP are tightly coupled.[30] In contrast, V-signal and functional CBV amplitude were tightly correlated ($R^2=0.9845$, $P=0.0001$). These findings suggest a decrease in vascular reactivity may underlie the attenuation of functional CBV responses following CSD. Error bars represent standard error.

responses were noticeably decreased ($t_1=0.034\pm0.002$, $t_2=0.028\pm0.002$, $t_3=0.027\pm0.002$, $t_4=0.033\pm0.002$, $t_5=0.034\pm0.002$, and $t_6=0.037\pm0.002$). A paired, two-tailed Student's t test revealed response amplitudes were significantly attenuated for the entire post-CSD imaging period, reaching a maximal attenuation at 20 to 30 min (Fig. 2).

Decreases in spontaneous vasomotor activity attributed to alterations in vascular reactivity following CSD have been previously reported.[32] To assess if similar decreases in vascular reactivity may have a played a role in the attenuation of functional CBV responses in our data we examined the change in spontaneous vasomotor activity following CSD. A low-frequency (0.1-Hz) oscillation in the reflected light signal results from spontaneous fluctuations in cerebral blood flow.[33,34] A power spectral density analysis of the 13-s prestimulus baseline in each trial following CSD revealed a significant peak in power centered at 0.1 Hz. Following CSD, the magnitude of this signal was significantly reduced, suggesting a decrease in spontaneous vasomotion and thus decreased vascular reactivity similar to that observed by Piper et al.[32] To compare how changes in vasomotor activity compared to functional CBV changes during the post-CSD period, we plotted the percent attenuation from baseline for each time bin on the same axis. Figure 3(a) shows that the two curves closely parallel each other. A least-squares regression analysis on the averaged data for the two variables showed functional CBV changes and spontaneous vasomotor activity were highly correlated ($R^2=0.9845$, $P<0.001$) following CSD.

ΣEP amplitude was decreased throughout the post-CSD period but to a lesser degree than functional CBV responses [Fig. 4(a)]. Pre-CSD ΣEP amplitude was 2.7 ± 0.11 mV. Post-CSD values were $t_1=2.47\pm0.11$ mV, $t_2=2.27\pm0.09$ mV, $t_3=2.09\pm0.08$ mV, $t_4=2.12\pm0.09$ mV, $t_5=2.15\pm0.09$ mV, and $t_6=2.24\pm0.10$ mV. Examination of the individual EP trains showed the waveform of an individual evoked response remained unchanged throughout the post-CSD period [Fig.

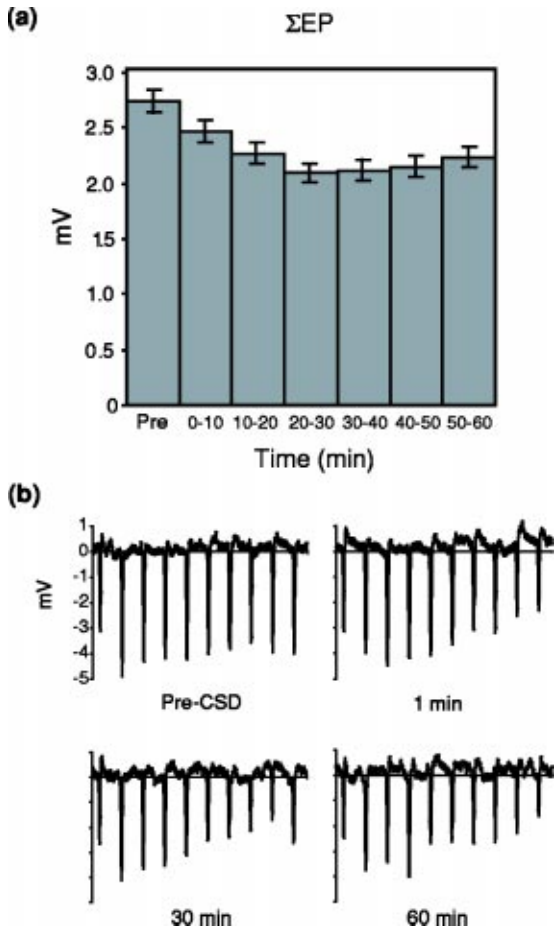

Fig. 4 Effect of CSD on ΣEP. (a) ΣEP was significantly attenuated following CSD. Values remained below baseline at 60 min following passage of CSD. Error bars represent standard error. (b) Raw evoked field potential traces from an electrical stimulus (2 s, 5 Hz, 1 mA) of 10 pulses in a single animal. Data from pre- and post-CSD trials at 1, 30, and 60 min are shown. The waveform of individual evoked responses was not significantly altered by CSD. Initial EPs were similar in amplitude to pre-CSD levels, however, responses later in the train appeared attenuated.

4(b)]. Within a stimulus train, initial EPs were similar in amplitude to pre-CSD levels, however, later responses appeared attenuated. To examine the relationship between changes in ΣEP and functional CBV signals during the post-CSD period we plotted the percent attenuation from baseline for each time bin for the two variables on the same axis. Figure 3(a) shows that in the first 30 min of the post-CSD period, peak CBV values were more strongly affected by CSD than those of ΣEP. Peak CBV was reduced by approximately 50%, whereas ΣEP amplitude showed a relatively minor attenuation. A least-squares regression analysis on the averaged data from all animals showed CBV and ΣEP were not well correlated during the post-CSD period ($R^2 = 0.073$, $P > 0.05$). Figure 3(b) shows the scatter plot of the data.

3.3 *Response Timing and Duration*

A summary of response onset, time to peak, and duration is listed in Table 1. Values significantly different ($P < 0.05$) from baseline values are denoted by a bold, italic font. Response onset times were not significantly different between pre- and post-CSD time points. Prior to CSD induction, responses began 1.2±0.1 s after stimulus onset. Similar onset times were noted for post-CSD time points. Time-to-peak, however, was significantly affected by CSD. Pre-CSD activations peaked 3.4±0.1 s after stimulus onset, while post-CSD activations peaked approximately 1 s earlier. No significant increase in time to peak was observed throughout the post-CSD period. CSD also markedly reduced response duration. Pre-CSD responses lasted 9.0±0.2 s, while post-CSD period values were shortened on average by 3 s, reaching a minimum (5.6±1.0 s) 10 to 30 min post-induction. Values increased throughout the post-CSD period reaching a value of 6.7±1.0 s by 60 min; however, this value was significantly shorter than pre-CSD levels.

4 Discussion

4.1 *OIS Changes Associated with CSD*

CSD produces a four-phase optical profile. The two initial small-amplitude waves of decreased then increased reflectance appeared to roughly coincide with the negative deflection in the local field potential [Fig. 1(b)] suggesting initial reflectance changes may be generated by the cellular phenomena associated with the electrophysiological spread of CSD. In hippocampal slice, CSD produces biphasic reflectance changes coincident with a negative shift in the dc potential[14] that bear a striking resemblance to our data. The source of initial reflectance decreases following CSD induction has been attributed to decreases in light scattering as a result of activation-induced changes in cell swelling. In the preparation used here, decreases in light scattering would also produce a decrease in reflectance. While changes in blood volume could also affect light scattering and reflectance values in the same direction, studies[21,22] using intravascular fluorescent dyes indicate no early volume changes associated with CSD. The etiology of subsequent early reflectance increases remains unknown. Potential generators of this phase include changes in mitochondrial swelling, dendritic beading, or ultrastructural cellular changes induced by CSD; however, the role of any of

Table 1 Response timing and duration.

	Pre-CSD	t_1	t_2	t_3	t_4	t_5	t_6
Response onset (s)	1.2±0.1	1.1±0.2	1.3±0.6	1.1±0.2	1.3±0.6	1.4±0.6	1.3±0.4
Time to peak (s)	3.4±0.1	***2.4±0.5***	***2.3±0.5***	***2.4±0.5***	***2.1±0.4***	***2.4±0.5***	***2.6±0.5***
Response duration (s)	9.0±0.2	***5.7±0.8***	***5.6±1.0***	***5.6±1.0***	***5.9±1.3***	***6.0±1.2***	***6.7±1.0***

these factors is presently inconclusive. Future multimodal studies are required to elucidate the origins of the early reflectance increase.

Later, large-scale reflectance changes in the presented study are likely vascular in nature. Studies comparing blood volume dye signals with OIS changes at isosbestic wavelengths suggest the late decrease then increase in reflectance represents a short-term increase and prolonged decrease in blood volume.[22] Studies using flow-sensitive techniques show a similar large-amplitude increase then decrease in cerebral blood flow[8,18] (CBF).

4.2 *Effect of CSD on Functional Hemodynamic Activity*

These data show CSD has a marked long-term effect on functional CBV signals exhibiting a maximal effect 20 to 30 min following the passage of spreading depression. The source of these changes may be either vascular or neuronal in origin, or may involve an interaction of the two. Previous studies have shown a significant impact of CSD on global and local stimulus-induced cerebrovascular activity. Using a helium clearance technique, Lacombe et al. observed a long-lasting (~2 h) global hypoperfusion following CSD that reached a minimum (17% below baseline levels) at 20 min post-induction.[35] Possible mechanisms underlying this impairment in hemodynamic function are a persistent cortical vasconstriction[36] and/or a reduction of local vascular reactivity[37] for up to 75 min following CSD. Regulation of local, stimulus-induced perfusion changes is similarly disrupted. fMRI recordings from patients experiencing migraine with aura show a significant decrease in the BOLD response to visual stimulation during the aura with only partial recovery[20] after 15 min. Our findings of significant reductions in the duration and magnitude of functional CBV activity as well as decreased spontaneous vasomotor activity further illustrate the profound effect of CSD on cerebral hemodynamics. Despite the significant effect of CSD on vascular function, attenuation in local electrophysiological activity could also produce the changes in CBV amplitude and timing seen here. Under normal conditions, the amplitude of ΣEP and functional CBV activity are tightly correlated.[28] Significant reductions in evoked responses and electroencephalographic (EEG) activity have been observed[1,38] following CSD for 10–15 min. While CSD does reduce the magnitude of electrophysiological activations, this period is relatively short compared to the impact on perfusion-related activity. In this paper, the attenuation of ΣEP was minor compared to that of functional CBV. Likewise, the two were not well correlated during the post-CSD period. These findings suggest changes in ΣEP may have played a minor role in the long-term attenuation of functional CBV activity but that the effect is primarily a vascular phenomenon.

4.3 *Implications for Functional Brain Mapping*

Our findings have significant implications for the analysis of functional imaging data such as BOLD fMRI that utilize correlative techniques to identify stimulus-related changes in cortical perfusion activity. These methods calculate the correlation coefficient between each pixel's time course with a predicted or reference hemodynamic function. Activity in pixels with a significant correlation coefficient is assumed to be related to the stimulus. The success of such a technique to identify functional areas requires the choice of an appropriate reference hemodynamic function. Our data show the amplitude and time course of this function is significantly altered following CSD. Maps generated using a reference function for normal conditions may fail to identify areas whose activity is tied to the stimulus. To ensure the accuracy of functional maps generated in patients, such as migraineurs, where CSD may disrupt normal vascular function, modeling of the hemodynamic response under nonstandard conditions is necessary.

In addition to significantly disrupting the temporal profile of functional CBV activity, our results showed CSD disrupted neurovascular coupling for at least 1 h following CSD. The true duration of this uncoupling cannot be determined from these data as our recording time was limited, but since CBV showed only minimal recovery at 60 min it is likely the coupling relationship is altered for much longer. As the core assumption of all perfusion-based imaging tools is a tight neurovascular coupling the presented data suggest these techniques may underestimate the magnitude of the underlying neuronal activation if subjects are imaged within a certain window following CSD. Future investigations are required to determine the time to full recovery of perfusion signals and restoration of the neurovascular coupling relationship. Data from such experiments is essential to our understanding of functional brain activity under pathophysiological conditions related to CSD and to the accurate interpretation of perfusion-based imaging data.

5 Conclusion

CSD had a significant and long-term effect on the profile of functional changes in CBV. Signal amplitude, duration, and time to peak were significantly altered by CSD and showed little recovery of pre-CSD values 60 min following induction. A possible source of this disruption may be a decrease in vascular reactivity. In contrast, electrophysiological activity was attenuated to a lesser degree. An inspection of the relationship between CBV and ΣEP during the post-CSD period showed the two were not well correlated, suggesting CSD leads to neurovascular uncoupling for at least 1 h.

Acknowledgments

This work was supported by grants from the National Institutes of Health (MH52083).

References

1. A. A. P. Leão, ''Spreading depression of activity in the cerebral cortex,'' *J. Neurophysiol.* **7**, 359–390 (1944).
2. K. Ohta, R. Graf, G. Rosner, and W. D. Heiss, ''Calcium ion transients in peri-infarct depolarizations may deteriorate ion homeostasis and expand infarction in focal cerebral ischemia in cats,'' *Stroke* **32**(2), 535–543 (2001).
3. H. Oka, M. Kako, M. Matsushima, and K. Ando, ''Traumatic spreading depression syndrome: review of a particular type of head injury in 37 patients,'' *Brain* **100**, 287–298 (1977).
4. K. A. Hossman, ''Periinfarct depolarizations,'' *Cerebrovasc. Brain Metab. Rev.* **8**, 195–208 (1996).
5. K. Takano, L. L. Latour, J. E. Formato, R. A. Carano, K. G. Helmer, Y. Hasegawa, C. H. Sotak, and M. Fisher, ''The role of spreading depression in focal ischemia evaluated by diffusion mapping,'' *Ann. Neurol.* **39**(3), 308–318 (1996).

6. M. Lauritzen, ''Pathophysiology of the migraine aura. The spreading depression theory,'' *Brain* **117**, 199–210 (1994).
7. A. Gorji, ''Spreading depression: a review of the clinical relevance,'' *Brain Res. Rev.* **38**(1–2), 33–60 (2001).
8. M. Lauritzen and M. Fabricius, ''Real time laser-Doppler perfusion imaging of cortical spreading depression in rat neocortex,'' *NeuroReport* **6**(9), 1271–1273 (1995).
9. R. D. Piper and G. A. Lambert, ''Inhalational anesthetics inhibit spreading depression: relevance to migraine,'' *Cephalalgia* **16**(2), 87–92 (1996).
10. V. I. Koroleva and J. Bureš, ''Blockade of cortical spreading depression in electrically and chemically stimulated areas of cerebral cortex in rats,'' *Electroencephalogr. Clin. Neurophysiol.* **48**(1), 1–15 (1980).
11. R. C. Guedes, F. A. de Azeredo, T. P. Hicks, R. J. Clarke, and T. Tashiro, ''Opioid mechanisms involved in the slow potential change and neuronal refractoriness during cortical spreading depression,'' *Exp. Brain Res.* **69**(1), 113–118 (1987).
12. F. Vyskočil, N. Kříž, and J. Bureš, ''Potassium-selective microelectrodes used for measuring the extracellular brain potassium during spreading depression and anoxic depolarization in rats,'' *Brain Res.* **39**(1), 255–259 (1972).
13. A. Van Harreveld and S. Ochs, ''Electrical and vascular concomitants of spreading depression,'' *Am. J. Physiol.* **189**(1), 159–166 (1957).
14. M. Müller and G. G. Somjen, ''Intrinsic optical signals in rat hippocampal slices during hypoxia-induced spreading depression-like depolarization,'' *J. Neurophysiol.* **82**(4), 1818–1831 (1999).
15. P. J. Shen and A. L. Gundlach, ''Prolonged induction of neuronal NOS expression and activity following cortical spreading depression (SD): implications for SD- and NO-mediated neuroprotection,'' *Exp. Neurol.* **160**(2), 317–332 (1999).
16. A. A. P. Leão, ''Pial circulation and spreading depression of activity in the cerebral cortex,'' *J. Neurophysiol.* **7**, 391–396 (1944).
17. M. Lauritzen, M. B. Jørgensen, N. H. Diemer, A. Gjedde, and A. J. Hansen, ''Persistent oligemia of rat cerebral cortex in the wake of spreading depression,'' *Ann. Neurol.* **12**(5), 469–474 (1982).
18. M. Fabricius and M. Lauritzen, ''Transient hyperemia succeeds oligemia in the wake of cortical spreading depression,'' *Brain Res.* **602**(2), 350–353 (1993).
19. Y. Kuge, Y. Hasegawa, C. Yokota, K. Minematsu, N. Hashimoto, Y. Miyake, and T. Yamaguchi, ''Effects of single and repetitive spreading depression on cerebral blood flow and glucose metabolism in cats: a PET study,'' *J. Neurol. Sci.* **176**(2), 114–123 (2000).
20. N. Hadjikhani, M. Sanchez Del Rio, O. Wu, D. Schwartz, D. Bakker, B. Fischl, K. K. Kwong, F. M. Cutrer, B. R. Rosen, R. B. Tootell, A. G. Sorensen, and M. A. Moskowitz, ''Mechanisms of migraine aura revealed by functional MRI in human visual cortex,'' *Proc. Natl. Acad. Sci. U.S.A.* **98**(8), 4687–4692 (2001).
21. A. M. O'Farrell, D. E. Rex, A. Muthialu, N. Pouratian, G. K. Wong, A. F. Cannestra, J. W. Chen, and A. W. Toga, ''Characterization of optical intrinsic signals and blood volume during cortical spreading depression,'' *NeuroReport* **11**(10), 2121–2125 (2000).
22. A. M. Ba, M. Guiou, N. Pouratian, A. Muthialu, D. E. Rex, A. F. Cannestra, J. W. Chen, and A. W. Toga, ''Multiwavelength optical intrinsic signal imaging of cortical spreading depression,'' *J. Neurophysiol.* **88**(5), 2726–2735 (2002).
23. L. B. Cohen, ''Changes in neuron structure during action potential propagation and synaptic transmission,'' *Physiol. Rev.* **53**, 373–418 (1973).
24. R. D. Frostig, E. E. Lieke, D. Y. Ts'o, and A. Grinvald, ''Cortical functional architecture and local coupling between neuronal activity and the microcirculation revealed by *in vivo* high-resolution optical imaging of intrinsic signals,'' *Proc. Natl. Acad. Sci. U.S.A.* **87**(16), 6082–6086 (1990).
25. A. F. Cannestra, A. J. Blood, K. L. Black, and A. W. Toga, ''The evolution of optical signals in human and rodent cortex,'' *Neuroimage* **3**(3), 202–208 (1996).
26. S. M. Narayan, E. M. Santori, A. J. Blood, J. S. Burton, and A. W. Toga, ''Imaging optical reflectance in rodent barrel and forelimb sensory cortex,'' *Neuroimage* **1**(3), 181–190 (1994).
27. A. Grinvald, E. Lieke, R. D. Frostig, C. D. Gilbert, and T. N. Wiesel, ''Functional architecture of cortex revealed by optical imaging of intrinsic signals,'' *Nature (London)* **324**(6095), 361–364 (1986).
28. S. Sheth, M. Nemoto, M. Guiou, M. Walker, N. Pouratian, and A. W. Toga, ''Evaluation of coupling between optical intrinsic signals and neuronal activity in rat somatosensory cortex,'' *Neuroimage* **19**(3), 884–894 (2003).
29. M. Nemoto, S. Sheth, M. Guiou, J. W. Y. Chen, and A. W. Toga, ''Functional signal- and paradigm-dependent linear relationships between synaptic activity and hemodynamic responses in rat somatosensory cortex,'' *J. Neurosci.* **24**(15), 3850–3861 (2004).
30. M. Lauritzen, ''Relationship of spikes, synaptic activity, and local changes of cerebral blood flow,'' *J. Cereb. Blood Flow Metab.* **21**, 1367–1383 (2001).
31. A. C. Ngai, M. A. Jolley, R. D'Ambrosio, J. R. Meno, and H. R. Winn, ''Frequency-dependent changes in cerebral blood flow and evoked potentials during somatosensory stimulation in the rat,'' *Brain Res.* **837**, 221–228 (1999).
32. R. D. Piper, G. A. Lambert, and J. W. Duckworth, ''Cortical blood flow changes during spreading depression in cats,'' *Am. J. Physiol.* **261**(1), H96–H102 (1991).
33. A. G. Hudetz, R. J. Roman, and D. R. Harder, ''Spontaneous flow oscillations in the cerebral cortex during acute changes in mean arterial pressure,'' *J. Cereb. Blood Flow Metab.* **12**, 491–499 (1992).
34. J. E. Mayhew, S. Askew, Y. Zheng, J. Porrill, G. W. Westby, P. Redgrave, D. M. Rector, and R. M. Harper, ''Cerebral vasomotion: a 0.1-Hz oscillation in reflected light imaging of neural activity,'' *Neuroimage* **4**, 183–193 (1996).
35. P. Lacombe, R. Sercombe, J. L. Correze, V. Springhetti, and J. Seylaz, ''Spreading depression induces prolonged reduction of cortical blood flow reactivity in the rat,'' *Exp. Neurol.* **117**(3), 278–286 (1992).
36. M. Shibata, C. W. Leffler, and D. W. Busija, ''Pial arteriolar constriction following cortical spreading depression is mediated by prostanoids,'' *Brain Res.* **572**(1–2), 190–197 (1992).
37. M. Wahl, M. Lauritzen, and L. Schilling, ''Change of cerebrovascular reactivity after cortical spreading depression in cats and rats,'' *Brain Res.* **411**(1), 72–80 (1987).
38. J. Bureš, O. Burešová, and J. Křivánek, *The Mechanism and Applications of Leao's Spreading Depression of Electroencephalographic Activity*, Academia, Prague (1974).